



## Utilization of banana peel for the removal of benzoic and salicylic acid from aqueous solutions and its potential reuse

Pranav D. Pathak<sup>a</sup>, Sachin A. Mandavgane<sup>a,\*</sup>, Bhaskar D. Kulkarni<sup>b</sup>

<sup>a</sup>Department of Chemical Engineering, Visvesvaraya National Institute of Technology, Nagpur 440010, India, email: [pranavdpathak@gmail.com](mailto:pranavdpathak@gmail.com) (P.D. Pathak), Tel. +91 712 2801563; Fax: +91 712 2223969; email: [sam@che.vnit.ac.in](mailto:sam@che.vnit.ac.in) (S.A. Mandavgane)

<sup>b</sup>CSIR National Chemical Laboratories, Pune 411008, India, email: [bdk@ncl.res.in](mailto:bdk@ncl.res.in)

Received 6 January 2015; Accepted 11 May 2015

### ABSTRACT

We report on the adsorptive removal of benzoic acid (BA) and salicylic acid (SA) using banana peel (BP), an abundantly available agricultural waste material, for the first time. BP was characterized by proximate analysis, FT-IR, scanning electron microscopy, BET surface area, and XRF. The number of basic sites on BP ( $4.9 \text{ mmol g}^{-1}$ ) is relatively more than acidic sites ( $0.75 \text{ mmol g}^{-1}$ ). The Langmuir uptake capacity values obtained are  $6.62 \text{ mg g}^{-1}$  for BA and  $9.80 \text{ mg g}^{-1}$  for SA. A mechanism for binding acid molecule to the BP surface is proposed.

*Keywords:* Benzoic acids; Salicylic acid; Banana peel; Adsorption; Wastewater treatment

### 1. Introduction

Increase in industrial, agricultural and domestic activities have resulted in generation of large amount of wastewater. This water contains harmful pollutants which may include organic and inorganic impurities such as heavy metals, aromatic compounds, and dyes and pigments. Many of these pollutants are harmful to human health [1–3].

Benzoic acid (BA) and salicylic acid (SA) are aromatic organic compounds which becomes harmful to human beings beyond their threshold concentration level. BA is used in beverages, toothpastes, mouth-washes, cosmetics, and pharmaceuticals [4–6]. SA is used in skin-care ointments, creams, gels, and transdermal patches. It is also used as an intermediate compound in some dyes. Due to insufficient treatment

of wastewater, it has been detected in ppm level in water bodies [7–9].

Different methods are reported for treatment of wastewater contaminated with aromatic organic acids such as ion exchange, reverse osmosis, liquid extraction, distillation, bipolar membrane electrodialysis, and reactive distillation. These methods are not effective while handling dilute solutions. Adsorption is a simple method and has been employed for removal of organic carboxylic acids [3,10]. An organic adsorbent can be used as power generation fuel or as fermentable substrate after adsorption. In this study, banana peel (BP) is used to remove organic pollutants from dilute solution. The advantage of using bio-adsorbent is that there is no need of desorption as pollutant-laden adsorbent itself can be used for gasification [11].

Different adsorbents such as montmorillonite [1,3], activated carbon [8,12], bentonites [2], resins [13,14], silica [15], and polymers [16] have been used to

\*Corresponding author.

remove BA. High-area activated carbon cloth [17], natural zeolites, and clay [8] are used for adsorption of SA. Preparation and modification of these adsorbents are expensive. Additionally, the solvents used for the modification reaction are usually toxic, and the process of treatment of material is also complicated.

BP, a cellulose-based material having 5.36% hemicelluloses and 11.1% cellulose [18], is a significant component of agricultural and industry waste, and its additional use will be desirable. Banana is a widely grown tropical fruit. It is cultivated by more than 130 countries. Its production is the highest in the world after citrus fruits. India is the major producer of banana in the world. It contributes 27% of the world's production [19].

The use of agricultural and industrial solid wastes such as BP as adsorbents for removing impurities has been studied extensively [20]. Most studies on the adsorptive capacity of BP have however focused on the cationic adsorption such as dyes [21] and heavy metals [22–24]. Only a few studies for the adsorption of anionic compounds such as Acid Blue 25 [25], Acid Black 1 [26], and some phenolic compounds [27] have examined the use of BP. In addition, to best of our information, none of these studies address reuse of BP for removal of carboxylic acids.

Furthermore, the study of the adsorptive behavior of BA and SA on BP is of interest from an ecological consideration. In order to standardize this system, a careful exploration of its acid–base behavior along with the effect of adsorbent dose, pH, time, initial concentration, and temperature on adsorption has been studied. Additionally, equilibrium, kinetic, and thermodynamic studies have been carried out in batch process.

## 2. Materials and methods

### 2.1. Material and its preparation

BP was collected from the local fruit market, cut into small pieces, sun-dried, crushed, and passed through 100 mesh sieves. After this, the BP was washed thoroughly with double-distilled water to remove any physical impurity on the surface. This was then dried in an air oven at 343 K till the constant weight was attained, i.e., moisture is totally removed. After complete drying, the BP was stored in airtight bags for further use.

### 2.2. Instrumentation and characterization

The BET surface area of BP was determined by Smart Sorb 92/93, surface area analyzer. The elemental

analysis (XRF) of BP was determined by an elemental analyzer (PAN analytical, model no PW2403). FT-IR spectra of BP and acid-adsorbed BP were noted using KBr disk method (Shimadzu, IR-Affinity 1). Scanning electron microscopy (SEM) images of BP were obtained using the scanning electron microscope (JSM 7600F). The Elementer VarioMicro cube model was used for CHNS analysis of BP. UV–vis spectrophotometer (Shimadzu UV-1800) was used for BA ( $\lambda_{\max} = 272$  nm) and SA ( $\lambda_{\max} = 297$  nm) analysis. pH meter (Evetech Instrument model pH 2700) was used for measuring pH values of the solutions.

### 2.3. Chemicals

Chemical stock solutions of BA and SA (Fisher Scientific make) were separately prepared by dissolving precise quantities in double-distilled water. Solutions of various concentrations were prepared from stock solutions. Its pH was adjusted by adding 0.1 N HCl/NaOH. Fresh dilutions were prepared for each experimental run, and analytical-grade reagents were used in this study. Properties and chemical structure of BA and SA are given in Table 1. Structurally, the only difference between BA and SA is the presence of an extra ortho hydroxy (–OH) group in SA.

### 2.4. Batch experiments

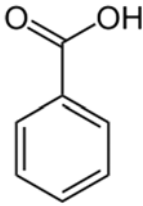
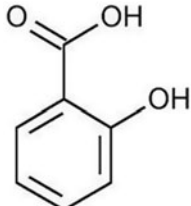
The adsorption of BA and SA with BP was studied using batch experiments with a view of understanding the effects of different parameters. These parameters included adsorbent dose, solution pH, time of contact, initial concentration, and temperature. A stock solution of 1,000 mg/L was first prepared and diluted as per the requirement of the experiment. The dilutions ranged from 50 to 400 mg/L. In each experiment, 50 ml of adsorbate of known concentration was mixed with desired quantity of BP in 100-ml conical flask. The mixture was agitated in a thermostatic shaker for 24 h at constant speed. The sample was then filtered, and the adsorbate concentration of the filtrate was analyzed by UV/VIS spectrophotometer.

The percent adsorption and adsorption capacity  $q_e$  (mg/g) at equilibrium was calculated as per the equations given below:

$$q_e = \frac{(C_0 - C_e)V}{w} \quad (1)$$

$$\% \text{ adsorption} = \frac{(C_0 - C_e)100}{C_0} \quad (2)$$

Table 1  
Selected properties for the BA and SA

Property	BA	SA
Molecular formula	C <sub>6</sub> H <sub>5</sub> COOH	C <sub>6</sub> H <sub>4</sub> (OH)COOH
Structure		
Molecular weight (g mol <sup>-1</sup> )	122.12	138.12
pKa value	4.202	2.97
Solubility of BA in water	2.9 g/L	1 g/L

### 3. Result and discussion

#### 3.1. Characterization of BP

BP was characterized using proximate analysis, CHNS analysis, XRF, BET surface area, FT-IR, and SEM. The surface charges and point of zero charge (pHpzc) of BP was also measured.

##### 3.1.1. Proximate and CHNS analysis

The analysis of dry BP was carried out to know the percentage of moisture, ash, volatile matter, C, H, N, and S. The results for proximate analysis are given in Table 2. The proximate analysis confirms high energy potential of BP (carbon: 40%; loss on ignition (LOI): 94%). The available nitrogen in the BP comes from 4–10% of crude protein present in BP [22,28]. The nitrogen present plays a vital role in anchoring acid molecule to the BP surface which has been discussed in detail in Section 4. Sulfur is present only in traces, and so, BP can be used for gasification.

Table 2  
Proximate analysis of BP

Parameter	Value (%)
Moisture	9.65
Dry matter	90.35
Ash	5.01
Volatile matter	85.26
Fixed Carbon	0.08
LOI	94.36
C	40.24
H	6.14
N	1.38
S	0.098
Surface pH	6.68

Table 3 shows the XRF analysis of the BP. This table reveals that BP contains Na, Si, Al, Cl, and traces of some metal elements. The high LOI of BP indicates that the volatile matter is present in large quantities.

##### 3.1.2. Surface area and elemental analysis of biosorbent

The surface area of BP was determined by BET method. The BET surface area of BP was found to be 0.65 m<sup>2</sup> g<sup>-1</sup>. This low surface area is probably due to the operational complexity of degassing lignocellulosic samples [26]. This low surface area of peels is a characteristic of carbonaceous materials [23].

##### 3.1.3. FT-IR analysis

In order to know the interactions between BP and the adsorbate molecule, it is necessary to identify the functional groups present on the surface of BP. FT-IR spectral comparison of the BP and acid-loaded BP identified the important binding sites (Fig. 1). The FT-IR spectra show the presence of hydroxyl, carboxylic, aldehyde, ester, amine, and amide groups on the surface of BP.

The stretching absorption bands at 3,441.01 cm<sup>-1</sup> represent –OH group in the adsorbent. This band wave number disappears in BA- and SA-loaded adsorbent. The broad stretching absorption bands centered at 3,269.34 cm<sup>-1</sup> represent –NH in the adsorbent. This band wave number shifts to 3,290.56 cm<sup>-1</sup> in BA-loaded adsorbent and 3,280.92 cm<sup>-1</sup> in SA-loaded adsorbent. The alteration in the wave numbers of the amino and hydroxyl group in FT-IR spectra indicates that these two groups are probably involved in the adsorption of BA or SA. The band obtained at around 2,916 cm<sup>-1</sup> is allocated to the stretching vibrations of

Table 3  
Elemental analysis of BP

Component	Na <sub>2</sub> O	MgO	Al <sub>2</sub> O <sub>3</sub>	SiO <sub>2</sub>	P <sub>2</sub> O <sub>5</sub>	SO <sub>3</sub>	K <sub>2</sub> O	CaO	TiO <sub>2</sub>	Cr <sub>2</sub> O <sub>3</sub>	MnO	Fe <sub>2</sub> O <sub>3</sub>	CuO	ZnO
%	0.17	0.17	0.07	0.99	0.11	0.24	0.03	3.06	0.47	0.01	0.02	0.24	0.01	0.02

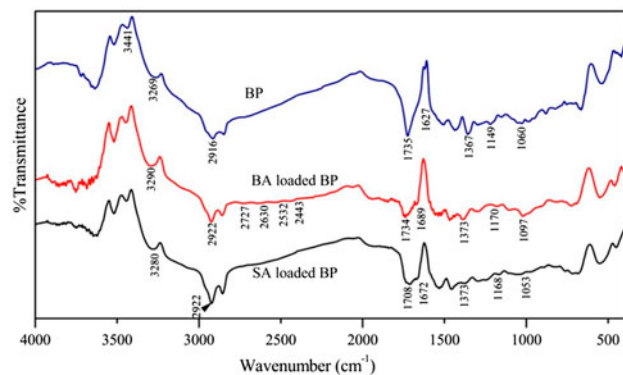


Fig. 1. FT-IR spectra of raw BP, BA-loaded BP, and SA-loaded BP.

CH<sub>3</sub> or CH<sub>2</sub> groups in carboxylic acid, and its bending vibration is at around 1,367 cm<sup>-1</sup> for BA. It shifted to 2,922 and 1,373 cm<sup>-1</sup> for BA- or SA-loaded BP. This indicates the presence of carboxylic acid after adsorption. The new peaks appearing at 2,727–2,443 cm<sup>-1</sup> in BA-loaded BP is related to O–H stretching of carboxylic acids. This shows that the acid is adsorbed on BP. The peak at 1,627 cm<sup>-1</sup> assigned to the C=C stretch of amide shifted to 1,689 cm<sup>-1</sup> for BA-loaded BP and to 1,672 cm<sup>-1</sup> for SA-loaded BP. This indicates the formation of new amide compounds. Carbonyl stretching band of unionized carboxylates of adsorbent was observed at 1,735 cm<sup>-1</sup> in case of BP. It is shifted to 1,734.01 and 1,708.93 cm<sup>-1</sup> for BA- and SA-loaded BP, respectively. The changes in the wave number values are in the range of 1,433–1,456 cm<sup>-1</sup> related to N–H bending and 1,060 cm<sup>-1</sup> related to C–N stretching frequencies. The shifting of these bands indicates the involvement of N–H of amines, C–O of amides, and carboxylic groups in the adsorption process. The biosorption peaks at 1,168–1,170 cm<sup>-1</sup> and 1,097–1,053 cm<sup>-1</sup> can be assigned to the C–C and C–N stretching vibrations, respectively of the BA- or SA-loaded adsorbents.

#### 3.1.4. SEM analysis of BP

A microporous structure was observed at a resolution of 25,000 × while taking the image of a particle size of 1 μm. Fig. 2 shows the typical micrograph of

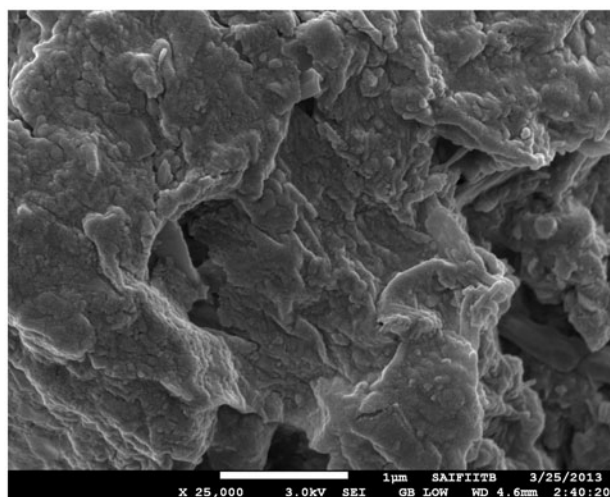


Fig. 2. Scanning electron micrograph of BP.

BP. The particles of BP are irregular in shape, and its surface displays a micro-rough texture. This shows very fine, millimeter or lesser size particles. Also, the pores present are considerably smaller than those can be observed in a typical SEM micrograph, and such micropores or mesopores might contribute to the major portion of surface area available for adsorption.

#### 3.1.5. Surface charges and point of zero charge

The knowledge of pH<sub>pzc</sub> prompts us to hypothesize on the ionization of functional groups and their interaction with ionic species present in solution. Point of zero charge, surface acidity, and basicity were determined using the method reported earlier [26,29].

The pH<sub>pzc</sub> value of BP is obtained at pH 5.36 (Fig. 3). The concentration of basic sites (4.9 mmol g<sup>-1</sup>) is relatively higher than the acidic sites (0.75 mmol g<sup>-1</sup>). This is the reason why BP can be categorized as an adsorbent with a basic character. Adsorption of cations is favored when pH > pH<sub>pzc</sub>, whereas the adsorption of anions is favored when pH < pH<sub>pzc</sub>. The specific adsorption of cations shifts to lower values, whereas the specific adsorption of anions shifts to higher values [30,31]. According to these findings, BP can be a low-cost adsorbent to uptake acid molecules from aqueous solution.

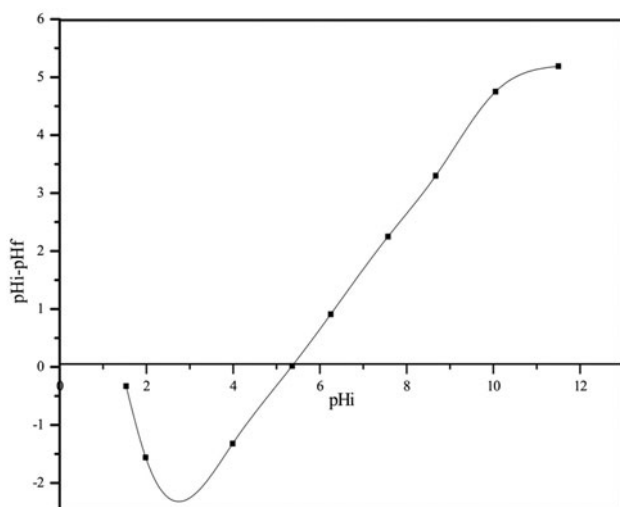


Fig. 3. Point of zero charge of BP.

### 3.2. Effect of adsorbent dosage

The effect of adsorbent dosage on removal of adsorbate at  $C_0 = 100$  mg/L was observed and plotted on a graph (Fig. 4). The graph shows the percentage removal of adsorbate against the adsorbent dosage (g/50 mL). The dosage of adsorbent varied from 0.2 g/50 mL to 4 g/50 mL keeping the concentration of BA and SA fixed. Theoretically, increasing the adsorbent dosage increases the adsorption. This ensures greater removal of adsorbate. This is due to the initial availability of more vacant spots for adsorption. During adsorption, a point was reached after which increase in adsorbent

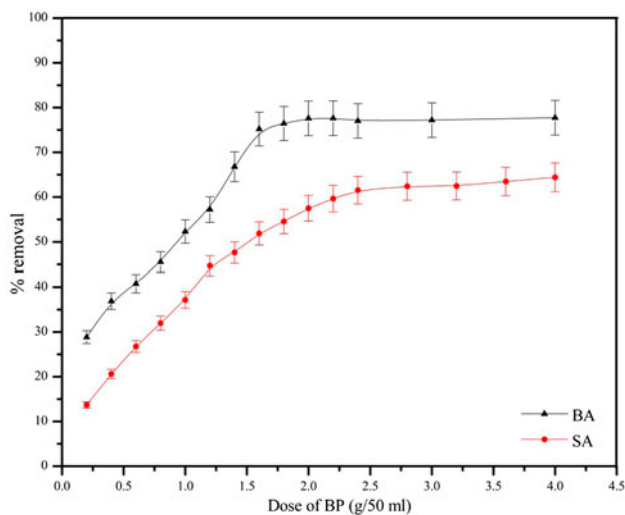


Fig. 4. Effect of dosage on the BA and SA removal ( $C_0 = 100$  mg/L,  $t = 15$  h,  $T = 303$  K, and  $V = 50$  mL).

dosage did not bring about any change in adsorption. This point was at 2 g/50 mL for BA and 2.4 g/50 mL for SA. These were selected as optimum dosages for adsorption of BA and SA. Fig. 4 shows that adsorption of BA was greater than SA. This is due to the repulsive forces of extra OH group present on BP. BA and SA are chemically almost identical. The only difference is an additional OH group in SA. The maximum adsorption achieved during the experiment was 77.59% for BA and 61.55% for SA.

### 3.3. Effect of pH

The pH value of a solution is an essential controlling parameter in the adsorption process [23]. The pattern of adsorption on plant materials is due to the active groups and bonds present on them [32]. Fig. 5 shows adsorption of BA and SA on BP in the pH range of 2–11. It was observed that the adsorption increased up to pH 3.68 and 3.3 for BA and SA, respectively. It was also observed that adsorption of BA and SA decreased when pH was further increased.

The surfaces had a positive charge when the pH value was lower than  $pH_{pzc}$ . The  $pH_{pzc}$  for BP is 5.36. BP is positively charged below this pH value. However, the natural pH of BA solution is 3.68. At this pH, BA is ~23% in its anionic form of benzoate ( $pK_a: 4.2$ ).

In general, it can be summarized that adsorption of BA is a summation of adsorption of dissociated and undissociated acid molecules. Undissociated molecules are attracted by hydrogen bonding, while dissociated,

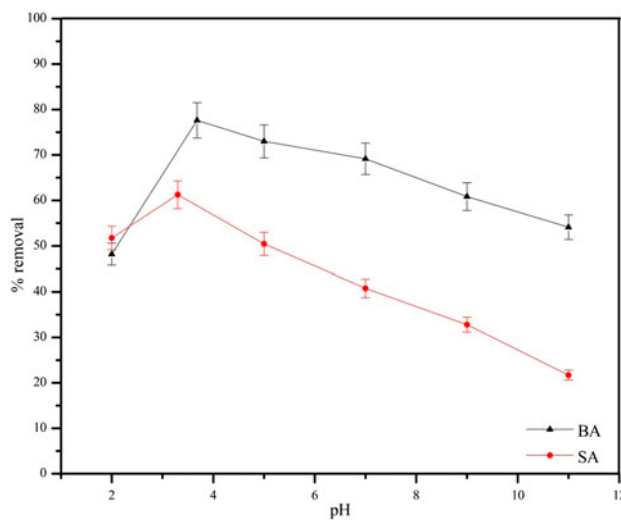


Fig. 5. Effect of pH on BA and SA removal ( $C_0 = 100$  mg/L,  $t = 15$  h,  $T = 303$  K, and  $V = 50$  mL).

i.e., ionic, molecules are by electrostatic force. At pH 2, solution contains ~99.4% BA molecules which are absorbed by hydrogen bonding [8,33,34]. The positive surface charges follow the trend  $\text{pH } 2.0 \gg 3.68 > 5.36$ . At higher pH ( $<5.36$ ), fraction of ion in solution increases, the difference between the solution pH and  $\text{pH}_{\text{pzc}}$  decreases, the relative positive charge on BP decreases, and hence, electrostatic force of attraction weakens. This results in reduction in (%) removal. Beyond pH 5.36, BP surface becomes negative and offers repulsion to benzoate ions present. Similar explanation is also valid for SA adsorption.

### 3.4. Effect of contact time

The effect of time of contact on BA and SA adsorption is given in Fig. 6. The figure shows that the removal of BA and SA increases gradually up to 12 and 14 h, respectively. There is no noteworthy change in removal after these durations of time. In addition, the adsorption of BA and SA stops completely after 20 h of contact. A more number of vacant sites on surface are available for removal during the early stage of sorption. The removal of acids is higher initially because a larger surface area is available for adsorption. Higher time of contact makes it tough for big-sized acid molecule to diffuse deeper into the BP. This happens because the mesopores are almost filled up after higher contact time and subsequently resist diffusion of acids [27]. This reduces the rate of adsorption with time.

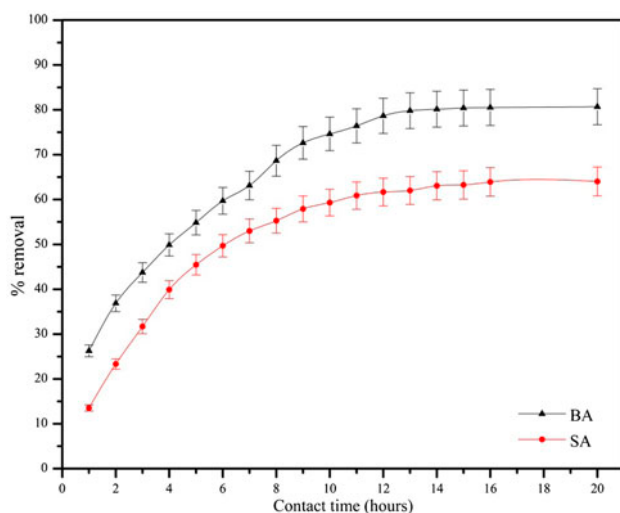


Fig. 6. Effect of contact time on BA and SA removal ( $C_0 = 100 \text{ mg/l}$ ,  $\text{pH}_{\text{BA}} = 3.68$ ,  $\text{pH}_{\text{SA}} = 3.3$ ,  $T = 303 \text{ k}$ , and  $V = 50 \text{ mL}$ ).

12 h of contact time for BA and 14 h of contact time for SA were chosen for subsequent batch experiments. At equilibrium, percentage removal achieved was 80.15 (BA) and 63.07 (SA).

### 3.5. Effect of initial concentration

Initial concentration provides the necessary driving force for adsorption. The initial concentration of acid is ranged between 50 and 400 mg/L. The maximum adsorbent dose for BA and SA was maintained at 2 g/50 ml and 2.4 g/50 ml, respectively. Variation of removal efficiency with initial concentration is shown in Fig. 7. The amount of adsorbate adsorbed per unit mass of BP increased with the increase of initial concentration. The percent adsorption of BA and SA reduced from 84.24 to 46.17% and 69.5 to 52.04% for the initial concentration of 50–400 mg/L, respectively. It is observed that amount of adsorbate molecules per unit mass of BP is higher. This created a greater driving force for promotion of more acid ions.

### 3.6. Effect of temperature

Adsorption was carried out at temperatures of 303, 313 and 323 K by varying initial concentrations between 50 and 400 mg/L for other optimum conditions. For BA, the optimum condition was pH 3.68, adsorbent dose 2 g/50 mL, and the optimum contact time 12 h. For SA, the optimum pH was 3.3 at an optimum adsorbent dose of 2.4 g/50 mL for a period of

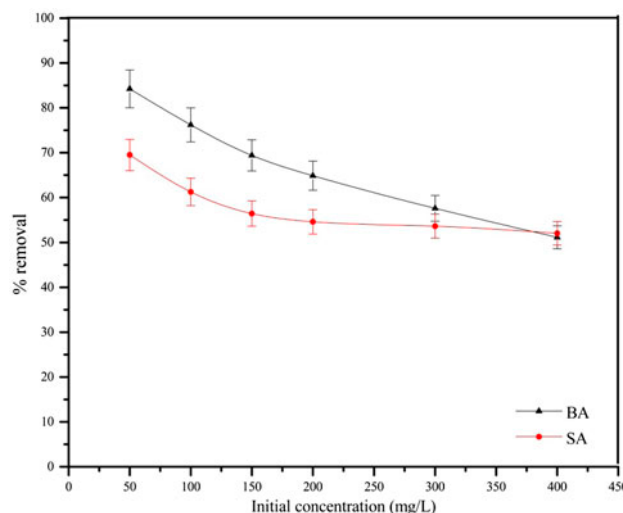


Fig. 7. Effect of initial concentration on BA and SA removal (for BA: pH 3.68, adsorbent dose 2 g/50 mL,  $t = 12 \text{ h}$ ; for SA: pH 3.3, adsorbent dose 2.4 g/50 mL, and  $t = 14 \text{ h}$ ).

14 h. The relation between equilibrium capacity ( $q_e$ ) and equilibrium concentration ( $C_e$ ) is shown in Fig. 8. The graph shows that increase in temperature and initial concentration of adsorbate correspondingly increased the equilibrium capacity ( $q_e$ ). This nature of curve shows that the reaction is more favorable at higher temperatures. This trend is in line with the reported literature [1].

### 3.7. Adsorption isotherm parameters

Adsorption isotherms are essential for the design of adsorption systems. Data obtained from isotherms inform about the amount of adsorbent necessary for removing a unit mass of impurity under the system conditions [35]. Langmuir and Freundlich isotherm equations were used in this study.

Langmuir adsorption model is based on monolayer adsorption on a homogeneous adsorbent surface. The Langmuir adsorption model can be expressed as follows:

$$\frac{C_e}{q_e} = \frac{C_e}{q_m} + \frac{1}{q_m K_L} \tag{3}$$

The values of  $q_m$  and  $K_L$  can be obtained by plotting  $C_e/q_e$  vs.  $C_e$ . The slope line is  $1/q_m$ , and  $y$ -intercept is  $1/(q_m K_L)$  [35].

The favorability of adsorption was predicted by interpreting the shape of isotherm [36]. The essential factor of the Langmuir isotherm is expressed by ‘ $R_L$ ’

which is a dimensionless constant. It is also known as equilibrium parameter or separation factor.  $R_L$  is calculated by Eq. (4).

$$R_L = \frac{1}{1 + C_0 K_L} \tag{4}$$

The parameter  $R_L$  specifies the shape of isotherm [37] as follows:

Value of $R_L$	Type of isotherm
$R_L = 0$	Irreversible
$R_L > 1$	Unfavorable
$0 < R_L < 1$	Favorable
$R_L = 1$	Linear

Freundlich adsorption model is established on multilayer adsorption on heterogeneous surfaces.

The Freundlich model [35] can be expressed as

$$\log q_e = \log k_F + \frac{1}{n} \log C_e \tag{5}$$

$K_F$  and  $n$  can be calculated by the linear plot of  $\log q_e$  vs.  $\log C_e$ .

Langmuir and Freundlich isotherm constants for the removal of BA and SA onto BP are calculated using Eqs. (3) and (5) and given in Table 4. The  $r^2$  value tells that Freundlich isotherm model fits better than the Langmuir isotherm model. The adsorption capacity of adsorbent increased with the increase in temperature. The adsorbent capacity ( $q_{max}$ ) is 6.62 and 9.80  $\text{mg g}^{-1}$  for BA and SA, respectively. These capacities are at a temperature of 323 K. The  $R_L$  values (Eq. (4)) for BA and SA are given in Table 4. These values ranged from 0 to 1. These values make the adsorption of BA and SA ions onto BP favorable. The Freundlich constant,  $K_F$ , determines the adsorption capacity of the adsorbent. Adsorbate is favorably adsorbed on the adsorbent if  $n > 1$ . The  $n$  values for BA and SA satisfy these conditions. This has been shown in Table 4. The higher the value of  $n$ , the stronger is the intensity of adsorption [38].

### 3.8. Kinetic parameters of biosorption

Kinetics of adsorption is important for explaining the effectiveness of an adsorbent. It tells us the uptake rate of adsorbate on adsorbent. This uptake rate physically controls the process of diffusion. Adsorption kinetics also defines the time of residence for adsorbate uptake at the interface of solid/solution.

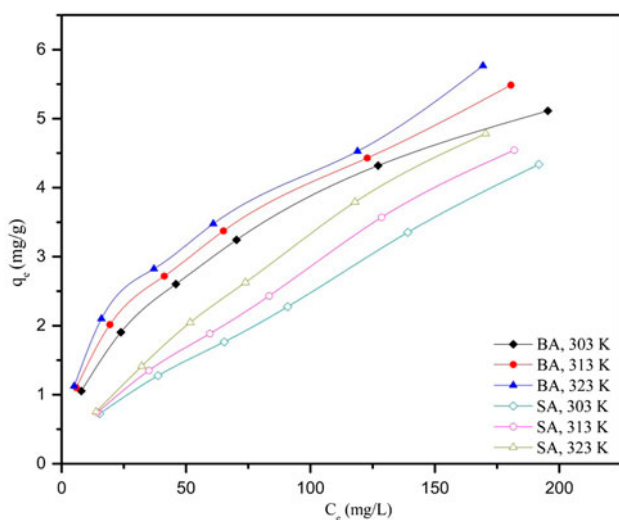


Fig. 8.  $q_e$  vs.  $C_e$  at different of temperature for BA and SA (for BA: pH 3.68, adsorbent dose 2 g/50 mL,  $t = 12$  h; for SA: pH 3.3, adsorbent dose 2.4 g/50 mL,  $t = 14$  h).

Table 4

Isotherm constants for the adsorption of BA and SA onto BP at various temperatures

	T (k)	Langmuir				Freundlich		
		$q_m$ (mg/g)	$K_L$ (L/mg)	$R_L$	$r^2$	$K_F$ (L/g)	$n$	$r^2$
BA	303	6.37	0.0177	0.360	0.976	0.39	2.02	0.998
	313	6.49	0.0215	0.317	0.960	0.49	2.18	0.998
	323	6.62	0.0248	0.287	0.952	0.57	2.25	0.993
SA	303	8.69	0.0046	0.685	0.779	0.10	1.42	0.991
	313	9.00	0.0051	0.662	0.852	1.07	1.40	0.996
	323	9.80	0.0054	0.649	0.955	0.10	1.35	0.999

Kinetics of adsorption can be controlled by different independent mechanisms. These mechanisms can act in series or in parallel. They include bulk diffusion, external mass transfer (film diffusion), intra-particle diffusion, and chemisorption (chemical reaction) [35].

Various kinetic models, such as the Lagergren-first-order, pseudo-second-order, Elovich, and intra-particle diffusion were used to understand biosorption kinetics. The Lagergren-first-order kinetic model equation [39,40] is given by Eq. (6).

$$\ln(q_e - q_t) = \ln q_e - k_1 t \quad (6)$$

The pseudo-second-order kinetic model equation [39,40] is given by Eq. (7).

$$\frac{t}{q_t} = \frac{1}{k_2 q_2^2} + \frac{t}{q_2} \quad (7)$$

The Elovich equation [40] is given by Eq. (8).

$$q_t = \frac{1}{\beta} \ln(\alpha\beta) + \frac{1}{\beta} \ln t \quad (8)$$

The Lagergren-first-order, pseudo-second-order, and Elovich kinetic models cannot recognize the diffusion mechanism. So intra-particle model was used for diffusion mechanism.

The intra-particle diffusion equation [41,42] can be written as Eq. (9):

$$q_t = k_{id} \cdot t^{\frac{1}{2}} + C \quad (9)$$

If the plot of Weber–Morris ( $q_t$  vs.  $t^{0.5}$ ) gives a straight line, then the adsorption process is controlled by intra-particle diffusion alone. However, two or more steps are involved in the adsorption–desorption process if it exhibits multi-linear plots [42].

The kinetic parameters are given in Table 5. The  $r^2$  values show that pseudo-second-order model fitted for SA ( $r^2 = 0.99$ ), while pseudo-first-order model ( $r^2 = 0.99$ ) fitted for BA.

The Elovich equation assumes that the active sites present on the adsorbent are heterogeneous in nature. This means they display different activation energies for chemisorption [40].

The intra-particle diffusion model is shown in Fig. 9. In the figure,  $q_t$  plotted against  $t^{1/2}$  shows multi-linear nature. Webber and Morris specified that intra-particle diffusion would exhibit a linear relationship when  $q_t$  is plotted against  $t^{1/2}$ . Diffusion would be controlling the rate of adsorption, provided this

Table 5  
Kinetic parameter of adsorption

Kinetic parameter	BA	SA
Pseudo-first-order		
$K_1$ (L min <sup>-1</sup> )	0.29	0.28
$Q_e$ (mg g <sup>-1</sup> )	1.68	1.45
$R^2$	0.956	0.996
Pseudo-second-order		
$K_2$ (g mg <sup>-1</sup> min <sup>-1</sup> )	0.07	0.08
$Q_e$ (mg g <sup>-1</sup> )	2.76	2.98
$R^2$	0.994	0.992
Elovich model		
$\alpha$ (mg g <sup>-1</sup> min <sup>-1</sup> )	1.51	0.75
$\beta$ (g mg <sup>-1</sup> )	1.84	2.31
$R^2$	0.979	0.991
Webber–Morris intra-particle diffusion model		
$k_{id 1}$ (mg g <sup>-1</sup> min <sup>-1/2</sup> )	0.59	0.55
$k_{id 2}$ (mg g <sup>-1</sup> min <sup>-1/2</sup> )	0.57	0.35
$k_{id 3}$ (mg g <sup>-1</sup> min <sup>-1/2</sup> )	0.31	0.15
C1	0.08	–
C2	0.10	0.18
C3	0.85	0.77
$r^2 1$	0.998	0.997
$r^2 2$	0.989	0.990
$r^2 3$	0.996	0.955

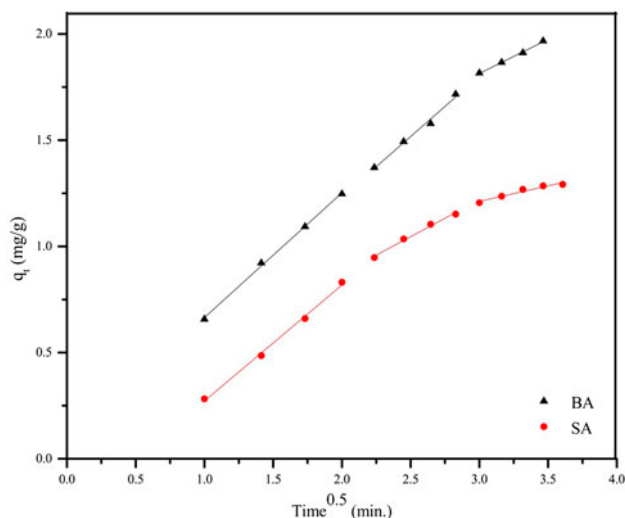


Fig. 9. Weber–Morris plot for BA and SA.

line passes through the origin. Fig. 9 was drawn to find out if the observed adsorption is controlled by intra-particle diffusion. Generally, the initial curve region (slope  $k_{id}$  1) represents the external surface adsorption in which the adsorbate diffuses from the solution to the outer surface of the adsorbent. In this step, the rate of adsorption is high. The second region (slope  $k_{id}$  2) represents macro-pore diffusion where the intra-particle diffusion is the rate-controlling step. However, if the line,  $q_t$  vs.  $t^{1/2}$  passed through the origin, then the particle diffusion would be the rate-controlling step. Finally, the third region (slope  $k_{id}$  3) is of micropore diffusion. This is the stage of equilibrium. Here, the intra-particle diffusion slows down and levels out as very less adsorbate concentration remains in the solution. It is also the stage where maximum adsorption is attained [35,43]. The diffusion rate parameters ( $k_{id}$ ) have been obtained from the slopes of straight lines. These have been given in Table 5. In Fig. 9, no line passes through the origin. This confirms to the non-zero values of intercept parameter  $C$ . This means there is early boundary layer resistance. It also means that intra-particle diffusion is involved in this process, but it is not the only rate-controlling step. The values of  $C$  are directly proportional to the thickness of boundary layer. It was found in the adsorption stage (Fig. 9) that values of  $C$  (Table 5) increased with time. This indicates the increase in the effect and thickness of the boundary layer.

### 3.9. Thermodynamic parameters of biosorption

Thermodynamic parameters include changes in the standard free energy ( $\Delta G^0$ ), enthalpy ( $\Delta H^0$ ), and

entropy ( $\Delta S^0$ ). These parameters, in relative to the adsorption process, are determined [42] using following Eqs. (10) and (11):

$$\Delta G^0 = -RT \ln K_d \quad (10)$$

$$\ln K_d = \frac{\Delta S^0}{R} - \frac{\Delta H^0}{RT} \quad (11)$$

The effect of temperature on the sorption of BA and SA on BP has been studied as discussed in Section 3.7. Enthalpy ( $\Delta H^0$ ) and entropy ( $\Delta S^0$ ) were determined from Van't Hoff's plot where  $\ln k_d$  was plotted against  $1/T$ .  $\Delta H^0$  gives the strength of bonding between the adsorbate and the adsorbent surfaces. The thermodynamic parameters of BA and SA are listed in Table 6. The positive values of  $\Delta S^0$  represent increased randomness at the interface of solid/solution.

The Gibbs free energy of adsorption is negative as predictable for spontaneous process.  $\Delta G^0$  decreases when the temperature is increased. This increases the adsorption of BA and SA on BP. This means that at higher temperatures, the adsorption is also higher. Since the adsorption is endothermic, the process of adsorption is spontaneous due to positive entropy change. Generally, the adsorption process is exothermic. However, in the above experiment, the adsorption is endothermic. This confirms that it has resulted in chemisorption. The increased adsorption capacity of BP at higher temperature may have been caused by the changes in pore size and/or activation of the BP surface.

### 3.10. Effect of structure of BA and SA on adsorption

BA and SA both contain carboxylate group. Structure similarity between two molecules is compared for the groups excluding  $-\text{COO}^-$  group of the molecules. SA contains an  $-\text{OH}$  substituent (at ortho position to carboxylate group) that has two lone pairs of electron on oxygen atom and provides additional negativity.

In aqueous acid solution, BP surface acts as positively charged. In addition to this, BP surface has

Table 6  
Thermodynamic parameters for BA and SA

Thermodynamic parameter	BA	SA
$\Delta G^0$ (kJ mol <sup>-1</sup> )		
303 K	-2,903.88	-1,155.54
313 K	-3,703.45	-1,600.26
323 K	-4,457.09	-2,001.88
$\Delta H^0$ (kJ mol <sup>-1</sup> )	303.73	176.43
$\Delta S^0$ (J mol <sup>-1</sup> K <sup>-1</sup> )	19.69	9.65

some active negative sites along with positive sites. In aqueous solution (pH 3.3), SA is singly charged anionic state (~67%) as its pKa value is 2.97. It shows lower adsorption due to electrostatic repulsive forces by the negative sites present on the BP surface. Since pKa value of BA is 4.2, in aqueous solution (pH 3.68) it is ~23% in anionic form. BA experiences lower electrostatic repulsion than SA because the number of ions of BA is less than that of SA at their respective natural pH. Hence, BA shows higher rate and extent of adsorption than SA. Some charge dipole interactions and dispersion are also expected to be effective in its adsorption.

### 3.11. Adsorption behavior of BA in water

BA in water is in neutral BA (~77%) and benzoate forms (~23%) at natural pH. The two forms absorb UV light at different  $\lambda_{\max}$  values: benzoate at 272 nm and BA at 218 nm. Since the  $\lambda_{\max}$  values of two species are different, their concentration can be measured simultaneously in a binary aqueous solution. This observation helps in understanding the change in concentrations of benzoate and BA during the period of 12 h. Similar situation is also true for SA in water, but analysis was not possible for it, due to closeness of  $\lambda_{\max}$  values of the neutral SA (299.5 nm) and ionic species (297 nm).

Concentration of BA in molecular form, benzoate anion, and the sum of the two at its natural pH are plotted separately as a function of time in Fig. 10. It is observed that the concentration of benzoate anion in aqueous solution decreases up to a minimum level

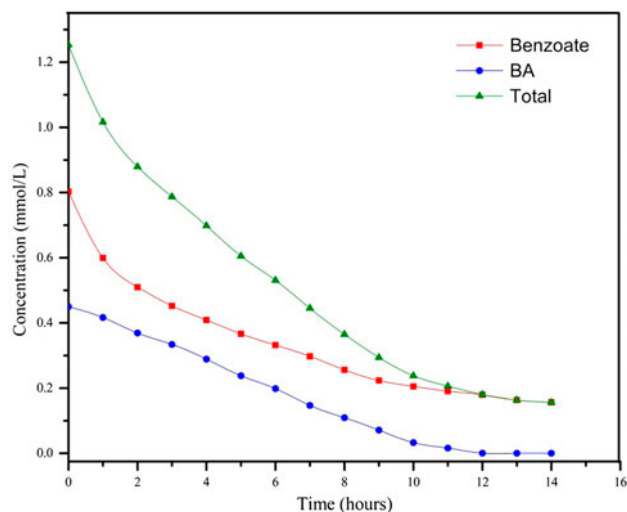


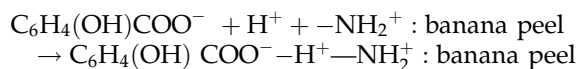
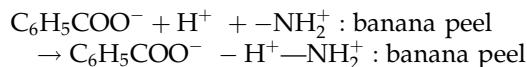
Fig. 10. Adsorption behavior of BA in water at natural pH.

over 12 h of adsorption period. This is due to the electrostatic attraction forces between benzoate anion and the positively charged BP surface. The decrease in neutral BA concentration is also seen. In the experiment, ~0.81 moles of BA were taken in an aqueous solution. At natural pH of solution, i.e., at 3.68, according to pKa value, ~23% BA gets dissociated. From Fig. 10, it is observed that at equilibrium (after 12 h), ~99% of BA contains neutral molecules and ~77% of benzoate ion is adsorbed on BP. The reduction in amount of BA is due to adsorption and partially due to dissociation. However, it is clear that adsorption of BA is more than the benzoate. BA gets adsorbed by weak hydrogen bonding, while benzoate by electrostatic force. It is observed that the adsorption of BA is a combined effect of electrostatic attraction and hydrogen bonding. However, hydrogen bonding dominates.

## 4. Proposed mechanism

It is difficult to know the mechanism which causes the adsorption of the organic compounds onto lignocellulosic waste. Their different origins prevent us from knowing the exact chemical structure and the functional groups present on the surface of the particle. The physicochemical characterization of the adsorbent surface, particularly the behavior of acid–base functional groups, may play a vital role in ionic interactions during the process [26].

The FT-IR results confirm the involvement of amine and hydroxyl groups in interaction during the adsorption of BA and SA on BP. The electrostatic force of attraction is an important factor between the positively charged BP surface, negatively charged benzoate ions, and succinate ions. The following reaction might be taking place:



This result indicates that the mechanism of ion exchange is involved in the process of adsorption.

Table 7 gives a comparison of adsorption capacity of BA and SA on different adsorbents. The adsorption capacity of BA and SA on BP is low. But the process has following advantages: (i) BP is easy and cheaply available. (ii) Both the adsorbent and adsorbate are biodegradable. BP is a potential source of renewable energy. The used adsorbent can be further used for

Table 7  
Adsorption results of BA and SA from the literature by various adsorbent

Acid	$q_{\max}$ (mg g <sup>-1</sup> )	Adsorbent	References
BA	27.17	HDTMA	[1]
	30.76	ODTMA	[1]
	20.80	OTMAC-bent	[2]
	22.03	Al(OH)-OTMAC-bent	[2]
	362.69 ± 18.32	High-area activated carbon cloth	[8]
SA	6.62	Banana peel	Present study
	418.51 ± 26.24	High-area activated carbon cloth	[8]
	1.483	Clays	[17]
	8.977	natural zeolites	[17]
	9.80	Banana peel	Present study

gasification for generation of power. (iii) Generally organic pollutants are chemically bonded to adsorbent surface, and safe disposal of the used adsorbent needs downstream processing. The proposed process is devoid of any downstream processing, but instead produces value-added products such as biogas and bio-char making the process eco-friendly. (iv) From food-processing industry's point of view, the solid waste generated, before charging in a gasifier, can be used to remove organic impurity from effluent. This will increase organic content of the feed to gasifier and will enrich the gas produced.

## 5. Conclusion

This work has used BP as a low-cost adsorbent. Its use to remove BA and SA from their aqueous solutions is extremely effective.

The following results were obtained during the experiment:

- (1) The result of FT-IR showed the adsorption of BA and SA on BP was achieved. The wave numbers of hydroxyl and amino groups on BP changed after the adsorption of BA and SA due to the interaction between the two. This confirms chemisorption.
- (2) The maximum adsorption capacities were obtained at pH 3.68 for BA and 3.3 for SA.
- (3) The Freundlich isotherm fits better than the Langmuir isotherm model.
- (4) The adsorption capacities ( $q_{\max}$ ) obtained at 323 K were 6.62 mg g<sup>-1</sup> for BA and 9.80 mg g<sup>-1</sup> for SA.
- (5) The adsorption of BA followed the pseudo-second-order kinetic model. The adsorption of SA followed the pseudo-first-order kinetic model.
- (6) Equilibrium time for BA and SA were 12 and 14 h, respectively.

- (7) The adsorption processes of BA and SA were spontaneous since the calculated values of  $\Delta G^0$  were negative. The positive values of  $\Delta H^0$  suggest that the adsorption was endothermic.
- (8) The proposed process is environmental friendly.

## Acknowledgments

The authors express their sincere gratitude to sophisticated characterization facilities provided by SAIF, IIT Bombay, JNARDDC, Nagpur, and department of applied chemistry, VNIT, Nagpur.

## Nomenclature

$C_0$	—	initial concentration of adsorbate (mg L <sup>-1</sup> )
$C_e$	—	equilibrium concentration of adsorbate in solution (mg L <sup>-1</sup> )
$V$	—	volume of the solution (L)
$w$	—	amount of adsorbent used (g)
$q_e$	—	adsorption capacity of adsorbate at equilibrium (mg g <sup>-1</sup> )
$q_t$	—	amounts of adsorbate on the adsorbent at any time $t$ (mg g <sup>-1</sup> )
$K_L$	—	Langmuir adsorption constant (L mg <sup>-1</sup> )
$q_m$	—	monolayer adsorption capacity of adsorbent (mg g <sup>-1</sup> )
$R_L$	—	dimensionless separation factor
$K_F$	—	Freundlich isotherm constant related to adsorption capacity ((mg g <sup>-1</sup> ) (L mg <sup>-1</sup> ) <sup>1/n</sup> )
$n$	—	Freundlich isotherm constant related to adsorption intensity
$q_{\max}$	—	maximum adsorption at monolayer coverage (mg/g)
$k_1$	—	rate constant of the Lagergren-first-order kinetic model (min <sup>-1</sup> )
$q_2$	—	maximum adsorption capacity for pseudo-second-order model (mg g <sup>-1</sup> )

$k_2$	— rate constant of pseudo-second-order model ( $\text{g mg}^{-1} \text{min}^{-1}$ )
$\alpha$	— initial adsorption rate for Elovich model ( $\text{mg g}^{-1} \text{min}^{-1}$ )
$\beta$	— desorption constant for the Elovich kinetic model ( $\text{mg g}^{-1}$ )
$k_{id}$	— intra-particle diffusion rate constant ( $\text{mg g}^{-1} \text{min}^{-1/2}$ )
$C$	— intercept for intra-particle diffusion rate constant
$T$	— absolute temperature (K)
$t$	— time (h)
$\Delta G^\circ$	— change in Gibb's free energy of adsorption (kJ/mol)
$\Delta H^\circ$	— change in enthalpy of adsorption (kJ/mol)
$\Delta S^\circ$	— change in entropy of adsorption (J/mol K)

## References

- [1] Y. Nuray, G. Rüya, K. Hülya, Ç. Ayla, Adsorption of benzoic acid and hydroquinone by organically modified bentonites, *Colloids Surf., A* 260 (2005) 87–94.
- [2] X. Xin, W. Si, Z. Yao, R. Feng, B. Dua, L. Yana, Q. Wei, Adsorption of benzoic acid from aqueous solution by three kinds of modified bentonites, *J. Colloid Interface Sci.* 359 (2011) 499–504.
- [3] L.-G. Yan, J. Wang, H.-Q. Yu, Q. Wei, B. Du, X.-Q. Shan, Adsorption of benzoic acid by CTAB exchanged montmorillonite, *Appl. Clay Sci.* 37 (2007) 226–230.
- [4] F.J.M. Mota, I.M.P.L.V.O. Ferreira, S.C. Cunha, M. Beatriz, P.P. Oliveira, Optimisation of extraction procedures for analysis of benzoic and sorbic acids in food-stuffs, *Food Chem.* 82 (2003) 469–473.
- [5] D. Shan, Q. Li, H. Xue, S. Cosnier, A highly reversible and sensitive tyrosinase inhibition-based amperometric biosensor for benzoic acid monitoring, *Sens. Actuators A* 134 (2008) 1016–1021.
- [6] C. Dong, W. Wang, Headspace solid-phase micro extraction applied to the simultaneous determination of sorbic and benzoic acids in beverages, *Anal Chim. Acta* 562 (2006) 23–29.
- [7] W.-L. Chau, C.-T. wang, K.-Y. Haung, T.-C. Liu, Electrochemical removal of salicylic acid from aqueous solutions using aluminum electrode, *Desalination* 271 (2011) 55–61.
- [8] E. Ayranci, O. Duman, Adsorption of aromatic organic acids onto high area activated carbon cloth in relation to wastewater purification, *J. Hazard. Mater. B* 136 (2006) 542–552.
- [9] M. Otero, C.A. Grande, A.E. Rodrigues, Adsorption of salicylic acid onto polymeric adsorbents and activated charcoal, *React. Funct. Polym.* 60 (2004) 203–213.
- [10] N. Yıldız, R. Gonulsena, H. Koyuncu, A. Calımlı, Adsorption of benzoic acid and hydroquinone by organically modified bentonites, *Colloids Surf., A* 260 (2005) 87–94.
- [11] J.Y. Tock, C.L. Lai, K.T. Lee, K.T. Tan, S. Bhatia, Banana biomass as potential renewable energy resource: A Malaysian case study, *Renewable Sustainable Energy Rev.* 14 (2010) 798–805.
- [12] C. Jia-Ming, C. Yi-Wen, Competitive adsorption of benzoic acid and p-nitrophenol onto activated carbon: Isotherm and breakthrough curves, *Water Res.* 37 (2003) 2347–2356.
- [13] K. Nobuhiro, U. Kohei, K. Naohiro, U. Yoshikuni, Exchange characteristics of monocarboxylic acids and monosulfonic acids onto anion-exchange resins, *J. Colloid Interface Sci.* 271 (2004) 20–27.
- [14] D.S. Farrier, A.L. Hines, S.W. Wang, Adsorption of phenol and benzoic acid from dilute aqueous solution onto a macroreticular resin, *J. Colloid Interface Sci.* 69 (1979) 233–237.
- [15] K. Spildo, H. Høiland, M.K. Olsen, Adsorption of benzoic and 4-heptylbenzoic acid on different silica substrates from organic and aqueous solution, *J. Colloid Interface Sci.* 221 (2000) 124–132.
- [16] F.-Q. Liu, J.-L. Chen, A.-M. Li, Z.-H. Fei, Z.-L. Zhu, Q.-X. Zhang, Properties and thermodynamics of adsorption of benzoic acid onto xad-4 and a water-compatible hypercrosslinked adsorbent, *Chin. J. Polym. Sci.* 21 (2003) 317–324.
- [17] R. Vesna, R. Nevenka, D. Aleksandra, A. Aline, The adsorption of salicylic acid, acetylsalicylic acid and atenolol from aqueous solutions onto natural zeolites and clays: Clinoptilolite, bentonite and kaolin, *Microporous Mesoporous Mater.* 166 (2013) 185–194.
- [18] N. Bardiya, D. Somayaji, S. Khanna, Biomethanation of banana peel and pineapple waste, *Bioresour. Technol.* 58 (1996) 73–76.
- [19] D. Mohapatra, S. Mishra, N. Sutar, Banana and its biproduct utilization, *J. Sci. Ind. Res.* 69 (2010) 232–329.
- [20] P.D. Pathak, S.A. Mandavgane, B.D. Kulkarni, Fruit peel waste a novel low cost bio adsorbent: A review, *Rev. Chem. Eng.* (in press).
- [21] K. Amel, M.A. Hassena, D. Kerroum, Isotherm and kinetics study of biosorption of cationic dye onto banana peel, *Energy Procedia* 19 (2012) 286–295.
- [22] J.R. Memon, S.Q. Memon, M.I. Bhangar, G.Z. Memon, A. El-Turki, G.C. Allen, Characterization of banana peel by scanning electron microscopy and FT-IR spectroscopy and its use for cadmium removal, *Colloids Surf., B* 66 (2008) 260–265.
- [23] R.S.D. Castro, L. Caetano, G. Ferreira, P.M. Padilha, M.J. Saeki, L.F. Zara, M.A.U. Martines, G.R. Castro, Banana peel applied to the solid phase extraction of copper and lead from river water: Preconcentration of metal ions with a fruit waste, *Ind. Eng. Chem. Res.* 50 (2011) 3446–3451.
- [24] J. Anwar, U. Shafique, W.U. Zaman, M. Salman, A. Dar, S. Anwar, Removal of Pb(II) and Cd(II) from water by adsorption on peels of banana, *Bioresour. Technol.* 101 (2010) 1752–1755.
- [25] M.G. Guiso, R. Biesuz, T. Vilariño, M. López-García, P.R. Barro, M. E. S. de Vicente, Adsorption of the prototype anionic anthraquinone, acid blue 25, on a modified banana peel: Comparison with equilibrium and kinetic ligand–receptor biochemical data, *Ind. Eng. Chem. Res.* 53 (2014) 2251–2260.
- [26] P. Carolyn, C. Elsa, U. Johana, M.M. Jesús, Eco-friendly technologies based on banana peel use for the decolourization of the dyeing process wastewater, *Waste Biomass Valorization* 2 (2010) 77–86.
- [27] M. Achak, A. Hafidi, N. Ouazzani, S. Sayadi, L. Mandi, Low cost biosorbent “banana peel” for the

- removal of phenolic compounds from olive mill wastewater: Kinetic and equilibrium studies, *J. Hazard. Mater.* 166 (2009) 117–125.
- [28] T. Tartrakoon, N. Chalearmsan, T. Veerasilp, U.T. Meulen, The nutritive value of banana peel (*Musa sapientum* L.) in growing pigs, in: *Sustainable Technology Development in Animal Agriculture*, Deutscher Tropentag, Berlin, 1999, pp. 1–4.
- [29] Y. Al-Degs, M.A.M. Khraisheh, S.J. Allen, M.N. Ahmad, Effect of carbon surface chemistry on the removal of reactive dyes from textile effluent, *Water Res.* 34 (2000) 927–935.
- [30] M. Iqbal, A. Saeed, S.I. Zafar, FTIR spectrophotometry, kinetics and adsorption isotherms modeling, ion exchange, and EDX analysis for understanding the mechanism of  $\text{Cd}^{2+}$  and  $\text{Pb}^{2+}$  removal by mango peel waste, *J. Hazard. Mater.* 164 (2009) 161–171.
- [31] V.C. Srivastava, I.D. Mall, I.M. Mishra, Characterization of mesoporous rice husk ash (RHA) and adsorption kinetics of metal ions from aqueous solution onto RHA, *J. Hazard. Mater. B* 134 (2006) 257–267.
- [32] A. Saeed, M. Sharif, M. Iqbal, Application potential of grapefruit peel as dye sorbent: Kinetics, equilibrium and mechanism of crystal violet adsorption, *J. Hazard. Mater.* 179 (2010) 564–572.
- [33] H. Hidaka, H. Honjo, S. Horikoshi, N. Serpone, Photocatalyzed degradation on a  $\text{TiO}_2$ -coated quartz crystal microbalance. Adsorption/desorption processes in real time in the degradation of benzoic acid and salicylic acid, *Catal. Commun.* 7 (2006) 331–335.
- [34] E. Ayranci, N. Hoda, E. Bayram, Adsorption of benzoic acid onto high specific area activated carbon cloth, *J. Colloid Interface Sci.* 284 (2005) 83–88.
- [35] C.O. Ijagbemi, M.H. Baek, D.S. Kim, Adsorptive performance of un-calcined sodium exchanged and acid modified montmorillonite for  $\text{Ni}^{2+}$  removal: Equilibrium, kinetics, thermodynamics and regeneration studies, *J. Hazard. Mater.* 174 (2010) 746–755.
- [36] C.O. Ay, A.S. Ozcan, Y. Erdogan, A. Ozcan, Characterization of *Punica granatum* L. peels and quantitative determination of its biosorption behavior towards lead(II) ions and acid blue 40, *Colloids Surf. B* 100 (2012) 197–204.
- [37] K.V. Kumar, K. Porkodi, Batch adsorber design for different solution volume/adsorbent mass ratios using the experimental equilibrium data with fixed solution volume/adsorbent mass ratio of malachite green onto orange peel, *Dyes Pigm.* 74 (2007) 590–594.
- [38] M.A. Ahmad, R. Alrozi, Removal of malachite green dye from aqueous solution using rambutan peel-based activated carbon: Equilibrium, kinetic and thermodynamic studies, *Chem. Eng. J.* 171 (2011) 510–516.
- [39] P.K. Tripathi, M. Liu, Y. Zhao, X. Ma, L. Gan, O. Noonan, C. Yu, Enlargement of uniform micropores in hierarchically ordered micro-mesoporous carbon for high level decontamination of bisphenol A, *J. Mater. Chem. A* 2 (2014) 8534–8544.
- [40] A.B.P. Marín, M.I. Aguilar, V.F. Meseguer, J.F. Ortuno, J. Sáez, M. Lloréns, Biosorption of chromium (III) by orange (*Citrus cinensis*) waste: Batch and continuous studies, *Chem. Eng. J.* 155 (2009) 199–206.
- [41] J.R. Memon, S.Q. Memon, M.I. Bhangar, A. El-Turki, K.R. Hallam, G.C. Allen, Banana peel: A green and economical sorbent for the selective removal of Cr(VI) from industrial wastewater, *Colloids Surf. B* 70 (2009) 232–237.
- [42] K. Totlani, R. Mehta, S.A. Mandavgane, Comparative study of adsorption of Ni (II) on RHA and carbon embedded silica obtained from RHA, *Chem. Eng. J.* 181–182 (2012) 376–386.
- [43] L.D. Fiorentin, D.E.G. Trigueros, A.N. Modenes, F.R. Espinoza-Quinones, N.C. Pereira, S.T.D. Barros, O.A.A. Santos, Biosorption of reactive blue 5G dye onto drying orange bagasse in batch system: Kinetic and equilibrium modeling, *Chem. Eng. J.* 163 (2010) 68–77.